To be submitted to
Nuovo Cimento

ISTITUTO NAZIONALE DI FISICA NUCLEARE
Laboratori Nazionali di Frascati

LNF-82/44(P)
28 Giugno 1982

S. Mobilio and L. Incoccia:

RADIAL DISTRIBUTION FUNCTION BY EXAFS: ASIMMETRY IN METALLIC GLASSES

Servizio Documentazione
dei Laboratori Nazionali di Frascati

INFN - Laboratori Nazionali di Frascati
Servizio Documentazione

LNF-82/44(P)
28 Giugno 1982

RADIAL DISTRIBUTION FUNCTION BY EXAFS: ASYMMETRY IN METALLIC GLASSES

Settimio Mobilio and Lucia Incoccia
PULS - Laboratori Nazionali dell'INFN, Frascati (Italy)

ABSTRACT

The authors discuss the informations on the radial distribution function (RDF) obtainable from EXAFS as compared with X-ray diffraction. The cases of Gaussian and non-Gaussian RDF's are illustrated showing how the Fourier transform (FT) of the experimental spectrum is connected with the RDF parameters in the two cases. The evidence of an asymmetric RDF in a metal glass, Fe_{80} B_{20}, is presented and discussed in detail.

1. - INTRODUCTION

The renewal of the interest towards EXAFS in the recent years is mostly due to the capability of this spectroscopy of investigating the local structure around an individual atomic species, irrespective of the aggregation state of the system. This unique property stimulated a large amount of experimental work in EXAFS especially in the cases where the traditional techniques failed[1]. These latters, like X-ray or neutron diffraction, require, generally speaking, the presence of a long range order in the system, and respond to the global structure of the sample as whole. Thus the most fruitful applications of EXAFS are whenever studying a disordered system, like amorphous materials, or systems very difficult to obtain in crystalline form, like biological molecules.

The ideal output of an EXAFS experiment on a disordered system would be a complete picture of the local static arrangement of atoms, including bond angles, and of their dynamical properties. As is well known, EXAFS alone cannot give all these information due principally to the one-dimensional nature of the absorption process at high energies of the photoelectron and to the inapplicability of the present single scattering theory to the low k region of the spectra. On the other hand EXAFS is highly sensitive to the radial distribution function of the nearest neighbours surrounding the absorbing atom which is often a crucial point to discriminate among different models of disorder. To fully exploit the potentiality of EXAFS, then, it is of great interest to understand how the experimental spectra are connected to the shape of the RDF, and what is the best way to extract such information in the data analysis. This point is particularly important when studying non-Gaussian RDF's, because there are many aspects of the data analysis that can hidden or mimick an asymmetry in the RDF.

The purpose of this work is to clarify some of these aspects, and to show how the presence of an asymmetric RDF has been detected in the case of metallic glasses.

In the first section we compare EXAFS and diffraction, discussing the complementarity of the two techniques. In section 2. and 3. we treat the case of Gaussian and non-Gaussian RDF's respectively, showing which information can be obtained in the two cases and in which way; in Section 4. an example of EXAFS analysis with an asymmetric RDF is discussed, illustrating the conceptual way leading to the use of the asymmetry in the analysis. The connection of the RDF with the interatomic potential is lastly briefly discussed.

2. - EXAFS VS. DIFFRACTION

Till now, the most widely used technique for structural investigations has been X-ray diffraction. It is particularly interesting then to analyze the informations one can get from EXAFS in comparison with diffraction. Generally speaking, when studying ordered systems, diffraction is the most powerful technique to obtain their complete three-dimensional map. In this case the role of EXAFS, which gives a one-dimensional view of the system, is important only in special cases. For example, when studying very complicate or dilute samples like proteins or solutions, EXAFS is able to reconstruct the local structure of the system around the one specific atom of interest in a relatively easy and direct way, while the same task in a diffraction experiment is very long and indirect[2]. A comparison between the two techniques is most appropriate in the case of disordered systems, where the stuctural information obtained is one-dimensional for both. Let us consider the 'total structure function' of diffraction:

$$i(s) = \sum_{ij} x_i x_j f_i f_j h_{ij}(s) \qquad (1)$$

where $h_{ij}(s)$ is the partial structure function of the atom pair i-j, related to the partial radial distribution function $g_{ij}(r)$ of the pair by:

$$h_{ij}(s) = 4\pi\varrho_o \int_o^\infty r\left[g_{ij}(r) - 1 \right] \sin(s \cdot r)\, dr \qquad (2)$$

$s = \frac{4\pi \sin\theta}{\lambda}$ is the momentum transfer between the incoming and outgoing photon, x_i is the atomic fraction of atom i, f_i representing the atomic form factor. Both techniques are related to the RDF by means of a sine Fourier Transform. It has to be underlined that in a diffraction experiment the total spectrum is built by the FT of $\frac{N(N+1)}{2}$ terms due to all the partial RDF g_{ij}, while in EXAFS, since one selects the absorbing center i, the sum is only over the subset of the N RDF of all the atomic species around the absorbing atom. This means that EXAFS gives a more direct picture of the single RDF, allowing a better test of the structural models[3]. A second point that has to be stressed is that the two techniques span two different k ranges. In fact, since EXAFS is a backscattering phenomenum the s value for a given energy of the photoelectron is $s = 2 \cdot k$ i.e. twice the momentum of the photoelectron itself. Moreover, diffraction spans tipically the region $s = 0 \div 16$ $\mathring{A}^{-1}$, the upper limit being due to experimental constraints.

EXAFS, on the other hand, lacks the informations at $s \lesssim 6$ $\mathring{A}^{-1}$ due to the failure of the single scattering theory, but reaches s values as large as 30 $\mathring{A}^{-1}$. As a consequence diffraction is most accurate in detecting long range order (~ 20 $\mathring{A}$) while EXAFS is highly sensitive to the nearest-neighbors environment. The last point has been interpreted recently as a limitation of EXAFS with respect to diffraction; actually the two techniques are complementary, since they probe different aspects of the RDF, and one has to make use of both to get a reliable picture of the RDF itself[5].

3. - RDF and EXAFS

Let us consider the expression of the EXAFS spectrum:

$$\chi(k) = \sum_j \frac{f_j(k,\pi)}{k} \int_o^\infty \frac{P_{ij}(r)}{r^2} \sin(2kr + \phi_{ij}(k))\, dk \qquad (3)$$

where $P_{ij}(r)=4\pi\varrho_o^2 g_{ij}(r)$ is the probability of finding an atom at distance r and the sum is over all different species of atoms in the sample. There are many problems in extracting $P_{ij}(r)$ from eq. (3). Indeed, $\chi(k)$ is not simply the Fourier Transform of $P_{ij}(r)$ due to the presence of both the backscattering amplitude function and the phase function. Restricting ourselves to the case of a single component system, if the backscattering amplitude is known either from theoretical calculation or from model compounds, it is possible to define $\chi'(k)$:

$$\chi'(k) = \frac{\chi(k).k}{f_j(k,\pi)} = \int_o^\infty \frac{P_{ij}(r)}{r^2} \sin(2kr + \phi_{ij}(k))\, dr \qquad (4)$$

$\chi'(K)$ is now the Fourier transform of $P_{ij}(r)$ provided the phase function is known and linear:

$$FT\ \ \chi'(k)\ \ \text{oc}\ P_{ij}\,(r + a_1/2)$$

where it has been supposed that $\phi(k) = a_o + a_1 k$[6].

This is no more true when the phases are not linear. But, due to the small curvature of the phase itself in the experimental k-range, the Fourier Transform is again a good picture of the $P_{ij}(r)$. But there is another problem that cannot be overcome. It comes out from the failure of the theoretical description that leads to the formula (3), when the photoelectron momentum k is smaller than 3 $\mathring{A}^{-1}$[7]. In this region, the wavelength of the photoelectron is greater than 2$\mathring{A}$: i.e. greater than the distances between the atoms of the systems. This implies that a single scattering formalism cannot describe the wavefunction of the outgoing electron: a multiple scattering approach has to be used, and the expression[3] does not hold anymore[8,9]. The lack of meaningful low momentum informations implies that RDF variations over distances greater than π/k_{min} cannot be detected by EXAFS[10].

Let us examine in some details the consequences of this last point in the cases of ordered and disordered systems.

a) Ordered Systems

In an ordered system like a crystal lattice, RDF is a sum of δ-like functions convoluted with the thermal motion:

$$P_{ij}(r) = \sum_{j=1}^{N} \delta(\bar{r} - \bar{r}_j) \otimes e^{-(r - r_j)^2/2\sigma_{ij}^2} \qquad (5)$$

where the sum is over all the atoms in the sample, and the origin is taken at the position of the absorbing atom.

Inserting this distribution function in eq. (3) one gets the well known classical EXAFS expression [7,11,12]:

$$\chi(k) = \sum_n \chi_n(k) = \sum_n \frac{N_n f_n(k,\pi)}{R_n^2} e^{-2\sigma_{in}^2 k^2} \sin(2kR_n + \phi_{in}(k)) \qquad (6)$$

In this case, the EXAFS spectrum is the sum of all the backscattered waves due to the atoms surrounding the

absorbing centre at different distances R_n.

Isolating a single component of the sum, in the ideal case $k_{min}=0$ and $\phi(k)=0$ the Fourier transform of

$$\chi'(K) = \frac{k\,\chi_n(k)}{f_n(k,\pi)}$$

is given by:

$$\text{Re}\ \ FT\chi'_n(k) = \frac{N_n\, i}{8\sigma R^2}\left[e^{-\frac{(R_n-r)^2}{2\sigma^2}}\ \text{erf}\ \frac{i(R_n-r)}{\sqrt{2\,2}} + e^{-\frac{(R_n+r)^2}{2\sigma^2}}\ \text{erf}\ \frac{i(R_n+r)}{\sqrt{2\sigma^2}}\right] \qquad (7)$$

$$\text{Im}\ \ FT\chi'_n(k) = \frac{N_n}{8\,\sigma\,R_n^2}\left[e^{-\frac{(R_n-r)^2}{2\sigma^2}} - e^{-\frac{(R_n+r)^2}{2\sigma^2}}\right];$$

The imaginary part, containing two Gaussian functions centered at $r=R_n$ and $r=-R_n$, represents the RDF for $r \geq 0$ with a replica in the region $r<0$. Moreover the imaginary part has a peak at $r=R_n$ where the real part is zero (Fig. 1). Fig. 2 shows that the magnitude of the Fourier Transform (FT), whose maximum coincides with the one

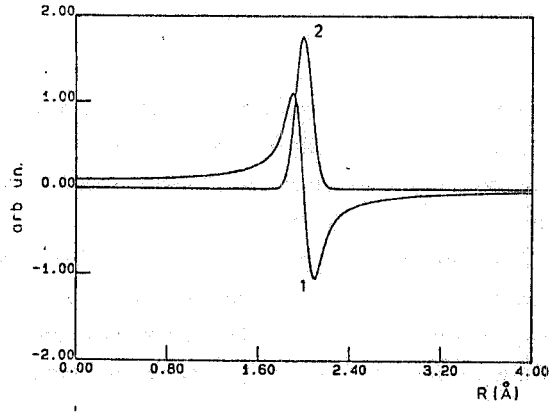

FIG. 1 - Real (1) and imaginary (2) part of the Fourier transform of $\chi(k)$.

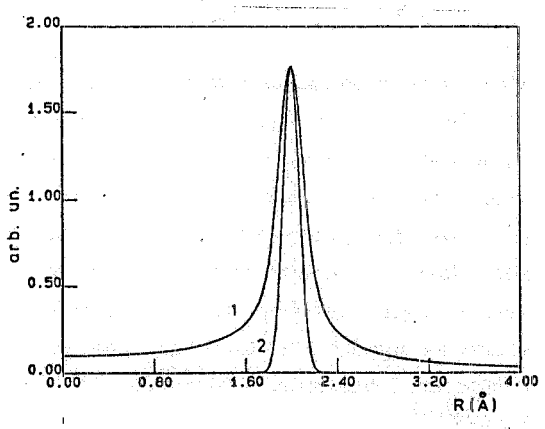

FIG. 2 - Magnitude (1) and imaginary (2) part of the Fourier transform of $\chi'(k)$

of the imaginary has a full width at half maximum (FWHM) W greater than the one of the RDF. It can be shown that the relation between W and σ is linear and can be approximated by:

$$W = \sqrt{2}\sigma \quad 2.96$$

Lastly the value of the maximum of the FT M is simply related to the coordination number by:

$$N_n = 8\sigma\ \ R_n^2\ \ M$$

So the analysis of the magnitude of the FT gives informations on the parameters of the RDF: peak position, coordination number and Debye Waller factors[12]. Introducing now a cutoff at $k=k_{min}$ and $k=k_{max}$, (since typically the spectrum is available between 3 Å^{-1} and 15 Å^{-1}) one gets[13]:

$$FT\ \chi'_n(k) = \frac{iN_n e^{-\frac{(R-r)^2}{2\sigma^2}}}{8\sigma R_n^2}\left(1 - \mathrm{erf}\left(\sqrt{2\sigma^2}\, k_{min} - i\frac{R-r}{\sqrt{2\sigma^2}}\right)\right) \qquad (8)$$

provided the value of k_{max} is sufficiently high so that $e^{-k_{max}^2\sigma^2} \simeq 0$ and the function $\mathrm{erf}(\sqrt{2\sigma^2}k_{max} + i(R-r)/\sqrt{2\sigma^2})$ can be approximated by its limiting values 1.

It is well known that the function erf(x+iy) exhibits oscillations whose main frequency is 2xy. As a consequence now the real and imaginary part of the FT show oscillations of the same frequency and neither the first nor the second describe the RDF (Fig. 3). But due to the $\pi/2$ shift of the oscillations in the two parts of the FT, its magnitude does not show them and still represents the RDF (Fig. 4). Thus the peak positions in the

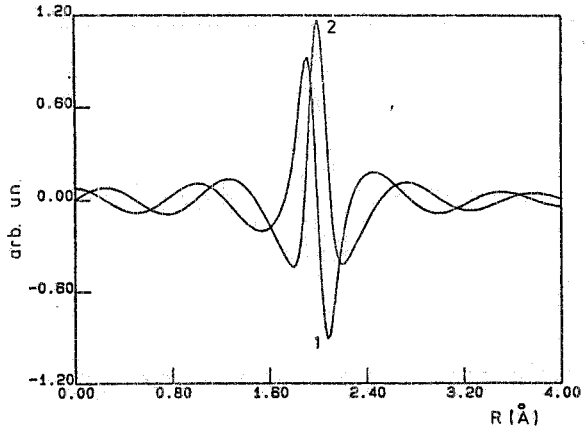

FIG. 3 - Real (1) and imaginary (2) part of the Fourier transform of $\chi'(k)$ in the case $k_{min}=3$ Å^{-1} and $k_{max} \to \infty$.

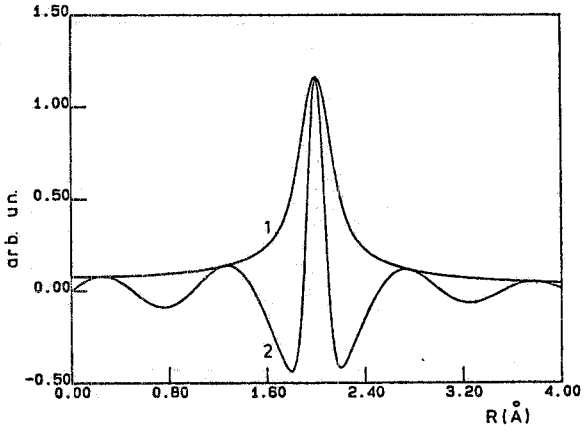

FIG. 4 - Magnitude (1) and imaginary (2) part of the FT of $\chi'(k)$ in the same case of Fig. 3.

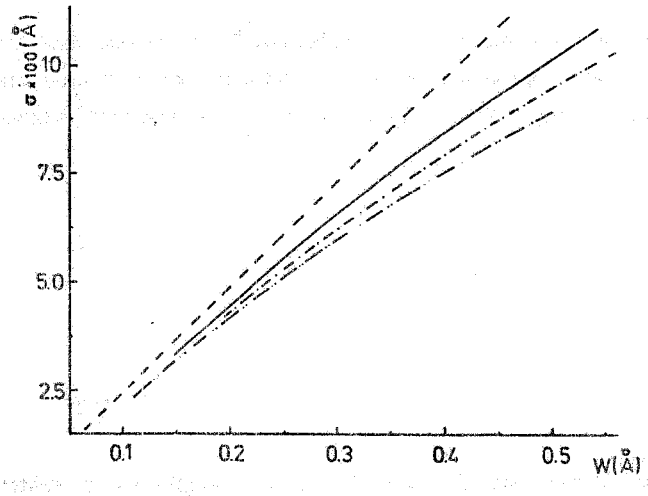

FIG. 5 - Behavior of σ as a function of the FWHM of the magnitude of the Fourier transform of $\chi'(k)$ for different values of k_{min}: 0 (——), 2 (——), 3 (-·-·-), 4 (··-··).

imaginary part and in the magnitude coincide, allowing again bondlength determinations from the FT. The relation between W and σ is now rather involved and is shown graphically in Fig. 5 for different values of k_{min}. Since the function $\sigma(W)$ has a monotonic behaviour, it is possible to determine the Debye-Waller factor from the FWHM. Again the coordination number is obtainable from the maximum of the FT M, by the relation:

$$N_n = 8\sigma R_n^2 \cdot M / \left(1 - \mathrm{erf}\left(\sqrt{2\sigma^2}\, k_{min}\right)\right)$$

In conclusion in an ordered system $k_{min} \neq 0$ is not yet a limitation. This can be understood since typical Debye-Waller factors are of the order of 0.05 Å, much smaller than $\frac{\pi}{k_{min}} \simeq 1$ Å. Also in k-space it turns

out that the damping term at k_{min} is $e^{-2k^2_{min}\sigma^2} \simeq 0.95$: no significant information has been lost in the region $0 \div k_{min}$.

The limitations of the above approach have been theoretically discussed by Greegor and Lytle[13], and are connected essentially with the difficulties in constructing the $\chi'(k)$ function from the experimental data since both the backscattering amplitude $f(k,\pi)$ and the inelastic losses are not accurately known[14]. But a systematic study of the feasibility of the above approach in experimental cases and a comparison with the usual procedure of analysis in k-space has not yet been done.

In actual spectra one has to take into account also the effect of the phase $\phi(k)$ in $\chi'(k)$. It has been shown by Lee and Beni[6] that if one knows $\phi(k)$, the function $\chi'(k)\, e^{-i\phi(k)}$ has the properties of $\chi'(k)$ of the ideal case $\phi(k)=0$ (Fig. 6). Indeed in this case the FT of $\chi'(k)\, e^{-i\phi(k)}$ is equal to (8) in the hypothesis of

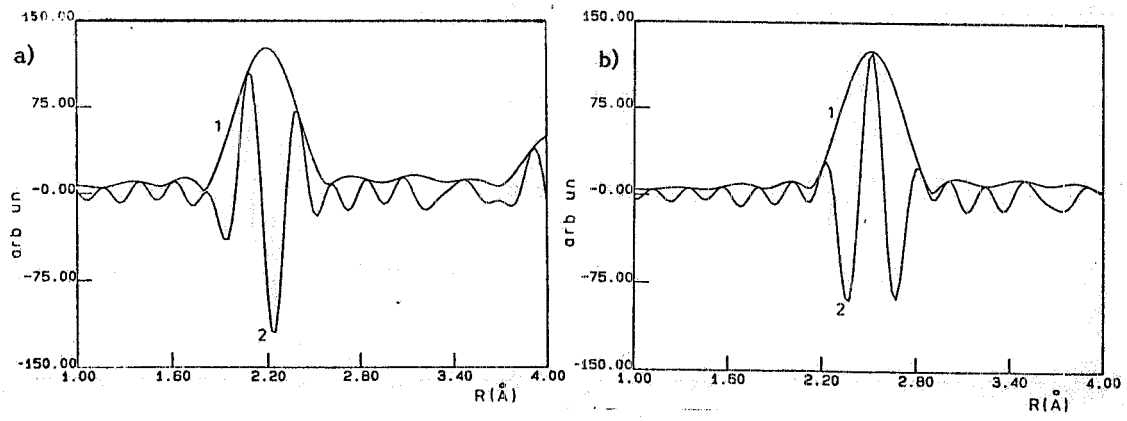

FIG. 6 - Magnitude (1) and imaginary (2) part of the FT of: a) $\chi'(k)$, b) $\chi'(k)e^{-i\phi(k)}$ in the case of pure Ni at LN_2T. The phase $\phi(k)$ was the experimental one deduced from the spectra.

neglecting, in the region of $r \geq 0$ the contribution to FT due to the tail of the replica of the RDF in the negative region of r, which now is different from the ideal case.

The phase function is generally determined either by using theoretical calculations[15] or by deducing the experimental phases from model compounds[16]. But in both approaches there are problems connected with the choice of the exact value of E_o, since the phases are unique only if the energy threshold E_o is specified[6]. Indeed a change in E_o will change the k value to k':

$$k' = \sqrt{k^2 + 0.263\, \Delta E_o} \qquad (9)$$

thus modifying the phase shift in the following way:

$$\phi'(k') = \phi(k) + 2\,(k' - k)\, R_n \qquad (10)$$

There are many factors that prevent the determination of the exact E_o value. There is no simple way to relate the features of the edge structure to the zero of the kinetic energy of the photoelectrons; moreover the effects of the chemical bonding[15] both in calculations and in phase transferability are neglected, the theoretical phases being referred to the unknown E_o energy of the muffin-tin calculations. In order to get a hint on the correct E_o

value one can treat it as a variable parameter, looking for some self-consistency in the analysis[6,17]. For example it was suggested to look for the value of E_o such that the imaginary part and the magnitude of the FT of $\chi'(k)\, e^{-i\phi(k)}$ peak at the same R-value[6].

b - Disordered Systems

A Gaussian RDF, although describing very well the physical situation when dealing with harmonic crystals, has been proved inadequate in the case of disordered systems. In such cases it is necessary to introduce a non symmetric RDF to completely understand the experimental data[18,19]. But the use of an asymmetric RDF in the EXAFS formulation introduces correcting factors in the amplitudes and phases so that the useful relations and criteria discussed don't apple anymore. In fact, as it has been pointed out by Eisenberger and Brown[18], the EXAFS spectrum for a general RDF is given by:

$$\chi(k) = \sum_i \frac{f_i(k,\pi)}{k} \sqrt{S_{ij}^2(k) + A_{ij}^2(k)} \quad \sin\left(2k\bar{r} + \phi_{ij}(k) + \sum_{ij}(k)\right) \qquad (12)$$

where:

$$S_{ij}(k) = \int_o^\infty P_{ij}(r + x) \cos 2kx\,dx \quad \text{and} \quad A_{ij}(k) = \int_o^\infty P_{ij}(r + x) \sin 2kx\,dx$$

and $\sum(k) = tg^{-1}(A(k)/S(k))$ is an additional "structural" phase term. The effect of $\chi(k)$ is such that the peaks in the imaginary part and magnitude of the FT of $\chi'(k)\, e^{-i\phi(k)}$ do not coincide even in the ideal case $k_{min}=0$ and $\phi(k)=0$ (Fig. 7). So the Lee and Beni criterium cannot be used to determine the E_o value. The E_o problem has to be solved in some other way. The presence of $\sum(k)$ moreover limits the phase transferability only to systems with the same RDF. The asymmetry strongly affects also the amplitudes: errors as large as 1 order of magnitude can be introduced in coordination numbers if asymmetry effects are neglected[18]. The correct procedure to extract information on RDF is to formulate a model of the distribution function on the basis of known physical properties of the system and to fit the parameters of the model to the experimental data. Still the most important limitation in EXAFS studies remains, namely the lack of meaningful information at $k \lesssim 3$ Å^{-1}. This implies that the slow varying features in RDF are smeared out by the truncation of the data at $k = 3$ Å^{-1}.

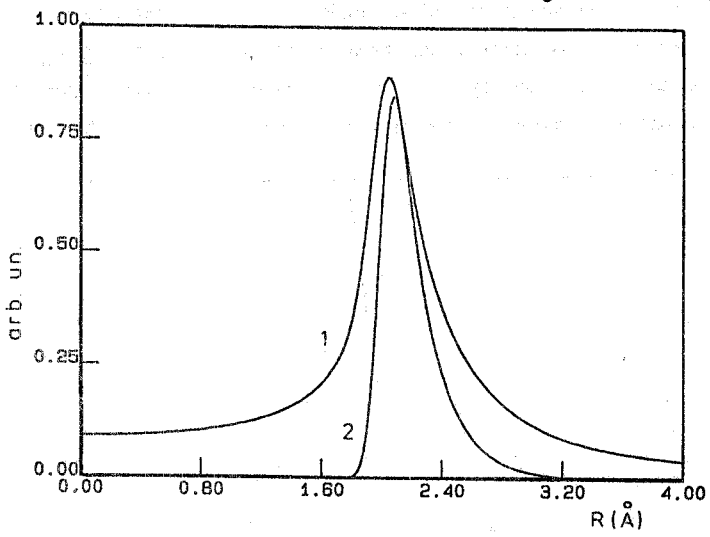

FIG. 7 - Magnitude (1) and imaginary (2) part of the FT of a $\chi'(k)$ simulated using an hard sphere model for the RDF.

This point is a strong limitation when studying disordered systems where structural models generally predict

smooth structures especially for the next neighbours shells. Let us consider, as an example, the case of a hard sphere system which is a good representation of physical systems like monoatomic liquids and amorphous metals. Computer simulations to get the 3-D most packed arrangement of one-diameter spheres[20], give a distribution function whose first peak can be well approximated by:

$$P(r) = \begin{cases} \frac{N}{\sigma_D} e^{-(r-r_j)/\sigma_D} & \text{for} \quad r \geqslant r_j \\ 0 & r < r_j \end{cases} \tag{13}$$

Inserting this P(r) into the EXAFS formula one gets[21]:

$$\chi(k) = \frac{f(k,\pi)}{k\sigma_D} \frac{N}{\sqrt{1 + 4k^2\sigma_D^2}} \sin\left(2k(\bar{r} - \sigma_D) + tg^{-1} 2k\sigma_D + \phi(k)\right) \tag{14}$$

where $\bar{r} = r_j + \sigma_D$ is the weighted mean of the distribution. The above $\chi(k)$ has a form quite different from the classical one and it is interesting to analyze its characteristics expecially in comparison with the diffraction results. As a matter of fact the additional phase term $\Sigma(k)$ in the k region spanned by EXAFS has a nearly constant value of about $\pi/2$ in disordered systems provided the value of σ_D is reasonably high ($\sigma_D = 0.2$ Å). Thus the effect of this term is only a constant phase shift over the whole spectrum and it is of no consequence in the peak position in the RDF. So, apart from the shift due to the scattering phase $\phi(k)$, one can see that the EXAFS frequency is $2k(\bar{r}-\sigma_D)=2kr_j$, i.e. the frequency of the sharp discontinuity in the RDF, the frequencies related to the smooth tail being in the lost region $k \leq k_{min}$. The diffraction interference function i(s), on the other hand, spans typically the region of low k where $\Sigma(k)$ can be approximated by its argument $2k\sigma_D$. So the response is mainly at the frequency due to $\bar{r}$ (Fig. 8). As a consequence, if the system is well represented by this

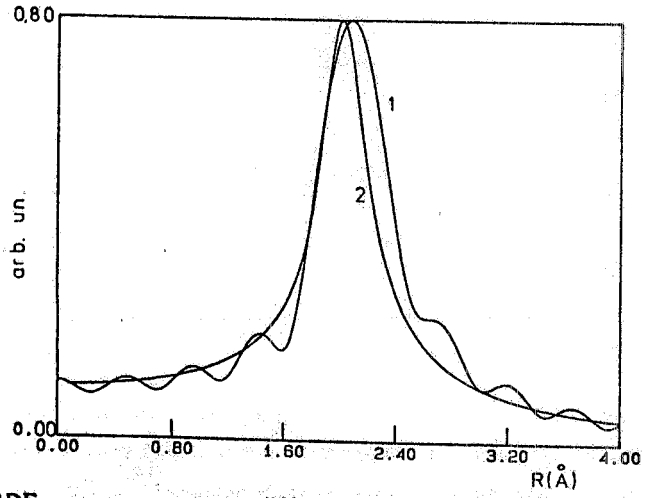

FIG. 8 - Magnitude of the FT of a spectrum simulated by using a hard sphere model for the RDF obtained transforming $\chi'(k)$ in the typical k range of diffraction (1) and of EXAFS (2).

RDF, one can expect a difference in peak positions between EXAFS and diffraction not explainable in term of scattering phase shifts. Contradictions between EXAFS results and the results obtained by other techniques, always have to suggest the introduction of an asymmetric RDF in the EXAFS analysis. This has been done in very few cases indeed. Eisenberger and Brown[18] studied crystalline Zn as a function of the temperature, finding a temperature dependence in the total phase. This, interpreted as an actual variation of the distances, leads to the inconsistent result of a contraction of 0.09 Å of the nearest neighbour distance in going from 20 K to 300 K,

versus the well knwon thermal expansion of 0.05 Å. This was explained by the authors as an asymmetry effect due to the structural phase term $\Sigma(k)$, whose variation as a function of the temperature is related to the deviation of the pair potential from harmonicity at high temperature. Crozier and Seary[22,23] extended this work to higher temperature also in the liquid phase, where they were able to determine the parameters of the pair potential by using a blip function as a model for the RDF. In the case of superionic conductors, Hayes et al.[19,24], using a fitting procedure in R space, introduced an RDF deduced from the excluded volume model. Only in this way the authors obtained a good reliability index explaining also the difference of their results with respect to the diffraction data. Finally, as it will be discussed in more detail in the next section, it has been shown[21,25] that in the case of T-N metallic glasses the asymmetry in the RDF is crucial in order to obtain important results from EXAFS data.

4. - ASYMMETRY IN METALLIC GLASSES: $Fe_{80}B_{20}$

T-N glassy metals are amorphous alloys obtained by rapid cooling from the melt composed by a transition metal (typically Fe, Ni, Pd...) and a metalloid (N, P, B). The composition range of these compounds is very narrow (around 80% of T and 20% of N). The interest towards these alloys is growing very rapidly because of their interesting properties for technological applications[25]. Their structural characteristics are not yet fully understood. The main features of their structure are explainable in term of a single-diameter hard spheres packing[20] representing the metal atoms, with the metalloids occupying the so-called Bernal holes left by the metal atoms, thus never being nearest neighbours independently from their ionic radii[27]. The last point has been directly probed by EXAFS measurements in Pd-Ge[28] and Ni-P[29]. Such completely random models for the structure of glassy metals are not fully satisfactory since they neglect any chemical order. A chemical ordering has been suggested to play an important role by Hayes et al.[28] on the basis of the rather narrow distribution of the metal atoms around the metalloid. This last point has been questioned by Boudreaux[30] by using a two-diameter spheres model interacting through a Lennard-Jones type potential. Anyhow for the first peak in the RDF, the distributions of the atoms around the metal is well represented by an RDF of the type[13] because of the hardness of the interacting potentials. This aspect has been fully checked by EXAFS in the case of $Fe_{80}B_{20}$ T-N met-glass[21,25]. In fact the use of a Gaussian RDF hindered a full understanding of the EXAFS data, while the introduction of a RDF of the type (13) can explain the experimental data, allowing the determination of the structural disorder parameter.

Fig. 9 shows the FT of an experimental spectrum of $Fe_{80}B_{20}$ at LNT taken at the PULS Laboratory in Frascati. If we now compare this FT with the expected one, build by using cristallographic data for the first Fe-

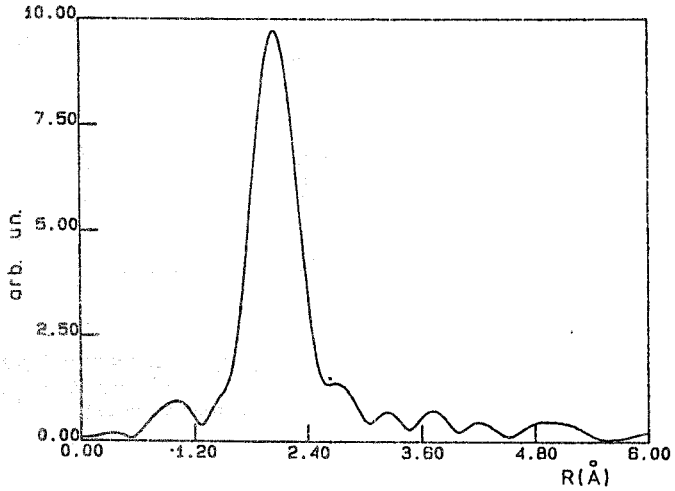

FIG. 9 - Magnitude FT of the spectrum of $Fe_{80}B_{20}$ at LN_2T.

Fe shell in $Fe_{80}B_{20}$ [31] and experimental phases for the Fe-Fe pair obtained by a two shells fitting on crystalline Fe, an impressive disagreement occurs in the peak position, the experimental one being 0.21 Å shorter than the theoretical one (Fig. 10). This difference cannot be explained by taking into account the presence of B in the sample at 2.05 Å. Indeed the total contribution of the B to the FT of the theoretical spectrum is completely negligible (Fig. 11). Another noticeable result is that the FT corrected by the Fe-Fe experimental phases doesn't show a coincidence in the peak position of the magnitude and imaginary part (Fig. 12). On the contrary, there is an overall phase shifth of about $\pi/2$. The application of the Lee and Beni criterium requires a shift of the edge

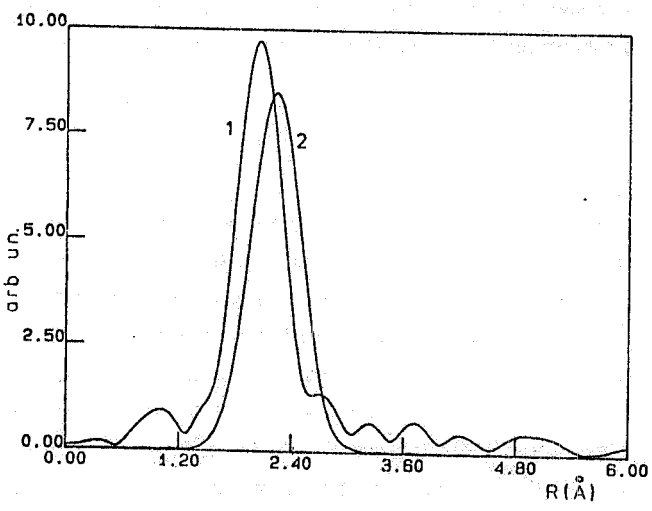

FIG. 10 - Comparison between the experimental (1) and theoretical (2) magnitude of the FT for $Fe_{80}B_{20}$. The theoretical one was obtained as discussed in the text.

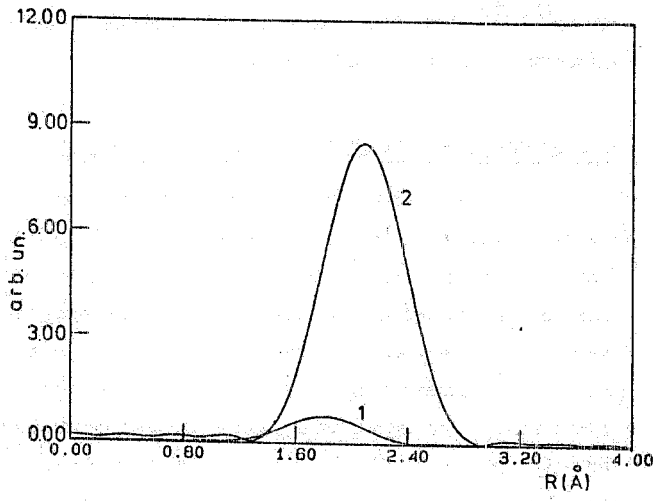

FIG. 11 - Contribution of the B atoms to the magnitude of the FT (1), compared with the one of the iron (2). All structure parameters are those of ref. (31).

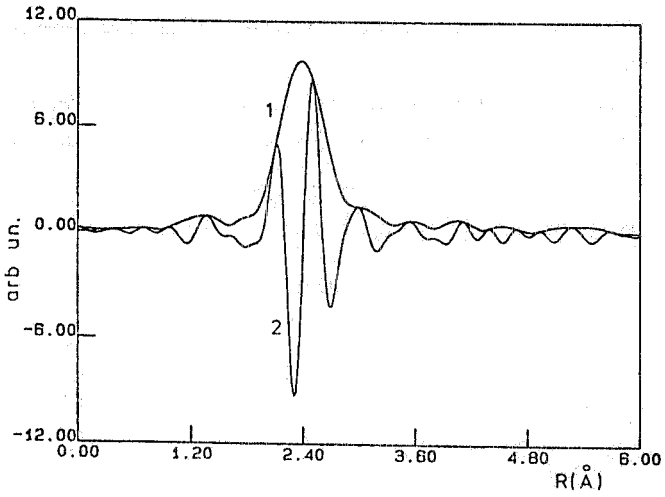

FIG. 12 - Magnitude (1) and imaginary (2) part of the FT of $\chi(k)$ of $Fe_{80}B_{20}$ corrected by the experimental phases.

energy of -32 eV or +15 eV in order to make the two peaks coincide: such high values of ΔE_o seem to be unlikely, since there is no physical reason to explain such a poor phase transferability for the Fe-Fe pair between pure Fe and $Fe_{80}B_{20}$. Furthermore even accepting such high E_o shifts, the experimental peak positions are at distances of 2.24 Å and 2.40 Å respectively, in contrast with both density and diffraction measurement.

Thus careful analys of the experimental data shows for $Fe_{80}B_{20}$ a contradiction between EXAFS and diffraction distances, and also a strong phase non-transferability effect.

All that suggests the introduction of an asymmetric RDF. Indeed, assuming an RDF of the kind (13) as a model for the Fe-Fe distribution, as already discussed, one expects exactly a structural phase term of $\pi/2$ and a difference between the next-neighbours distances obtained by EXAFS and diffraction. In order to check this hypothesis in a more quantitative way, we have fitted the phases of the experimental inverse Fourier transform of the first peak with the model provided by eq. 14. In order to avoid any effect due both to incorrect determination of the experimental amplitude of the EXAFS and to the correlation between the amplitude and the phase of the $\chi(k)$ due to the presence of the term σ_D in both, we have deduced the experimental function sin $\phi_{tot}(k)$ by dividing the inverse Fourier transform by its envelope function A(k). This function fitted in the k range 4÷12.5 $Å^{-1}$ to:

$$\sin (2 K \overline{R} + \phi(k) - 2 k\sigma_D + tg^{-1} (2 k.\sigma_D))$$

assuming for $\overline{R}$ the cristallographic value and σ_D and ΔE_o as variable parameters to be determined, gave the following results:

$$\sigma_D = 0.21 \pm 0.03 \text{ Å}$$

$$\Delta E_o = + 6.2 \text{ eV} \pm 1 \text{ eV}$$

with a global correlation coefficient on all parameters less than 0.3. As shown in Fig. 13 the experimental sine

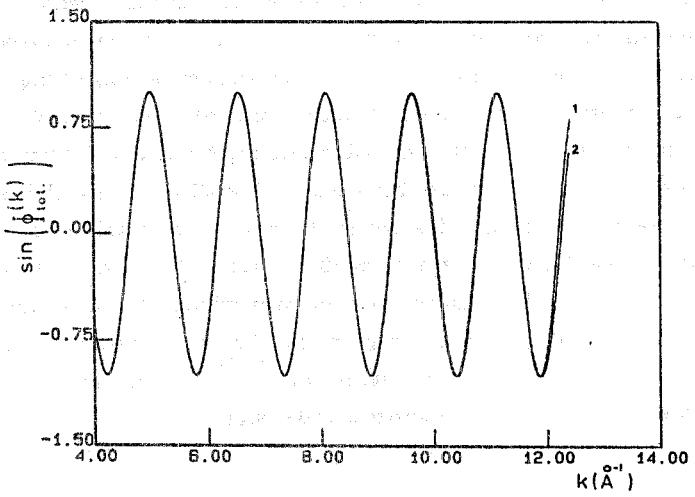

FIG. 13 - Experimental and fitted sin $\phi_{tot}(k)$: (0000) experimental curve (——) output of the fitting procedure.

function and the fitted one are completely undistinguishable over the k range available.

As for the amplitude parameters we fitted the experimental spectrum by keeping fixed the quantities determined by the previous fitting procedure, allowing only N are σ^2_{DW} to vary. Due to the smallness of the k-range available, the resulting parameters were strongly correlated (0.85), so there is need of an independent measurement of one of them. In our case, if one assume that the σ^2_{DW} of the Fe-Fe pair in $Fe_{80}B_{20}$ is the same as in pure iron[32] σ_{DW}=0.0026 Å, one gets for the coordination number the value:

N = 12. 4 ± 1.00 (Fig. 14)

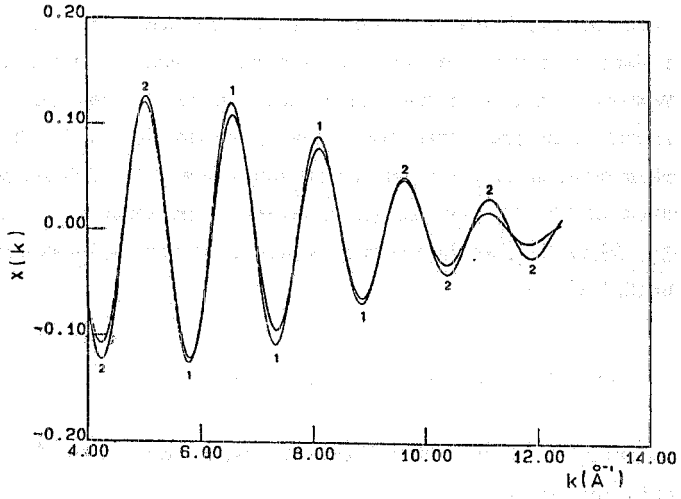

FIG. 14 - Experimental and fitted $\chi(k)$: (1) experimental curve, (2) output of the fitting procedure.

Thus the use of such a model for the RDF, allowed to determine the disorder parameters and the coordination number with high accuracy, thus explaining both diffraction and EXAFS data.

5. - CONCLUSIONS

The full determination of the radial distribution function is crucial in order to understand not only the structural properties of a system but also the interacting potential between the constituent atoms. This potential determine both the dynamical properties of the system and the structural ones, beeing related respectively to the atomic motion and to the statical equilibrium positions. Both the two main structural techniques X-ray diffraction and EXAFS, allows the determination of the Debye-Waller which, beeing related to the projected density of phonons[32], is a measure of the dinamics of a systems; they determine also the statical RDF. But in both cases the two techniques provide quite different informations, the X-ray diffraction being sensitive to the "absolute" motion of the atoms and to the smooth behaviour of the RDF, the EXAFS on the contrary, providing the relative motion of the atoms and the sharp feature of the RDF. Thus in all systems where there is a strong anharmonicity of the potential like high temperature or disordered systems, a comparative study is the unique way to fully understand the forces that build up the system. In particular the evidence of an asymmetry in the RDF is a way to show up the anharmonicity of the potential. The hard task of calculating the full potential parameters of the system, done only in few cases until now[22,23,24], will be the next step in EXAFS data analysis, in order to get more informations on the systems under study.

REFERENCES

(1) For a general review on EXAFS see, for example: P.A. Lee, P.H. Citrin, P. Eisenberger and B.M. Kinkaid, Rev. Mod. Phys. 53, 769 (1981).
(2) R. Caminiti, G. Licheri, G. Piccaluga, G. Pinna, Review in Inorganic Chemistry, 1, 333 (1979).
(3) T.M. Hayes, J. of Non Crystalline Solids, 31, 57 (1978).
(4) B.E. Warren, "X-ray Diffraction", AddisonWesley (1969).
(5) R.F. Pettifer, Proc. of the Daresbury Study Week-end, 28-29 March (1981), DL/SCI/R17 Daresbury Internal Report, pag. 57.
(6) P.A. Lee and G. Beni, Phys. Rev. B15, 2862 (1977).
(7) E.A. Stern, Phys. Rev. B10, 3027 (1974).
(8) P.A. Lee and J.B. Pendry, Phys. Rev. B11, 2795 (1975).
(9) J.B. Pendry, Proc. of the Daresbury Study Week-end, 28-29 March 1981, DL/SCI/R17 Daresbury Internal Report pag. 5.
(10) G.S. Brown, in: "Synchrotron Radiation Research" ed. by H. Winick and S. Doniach, Plenum Press, New York (1980).
(11) F.W. Lytle, D.E. Sayers and E.A. Stern, Phys. Rev. B11, 4825, (1975).
(12) D.E. Sayers, E.A. Stern and F.W. Lytle, Phys. Rev. Letters 27, 1204 (1971).
(13) R.B. Greegor and F.W. Lytle, Phys. Rev. B20, 4902 (1979).
(14) E.A. Stern, B.A. Brunker and S.M. Heald, Phys. Rev. B21, 5521 (1980).
(15) B.K. Teo and P.A. Lee, J. Am. Chem. Soc. 101, 2815 (1979).
(16) P.H. Citrin, P. Eisenberger and B.M. Kincaid, Phys. Rev. Letters 36, 1346 (1976).
(17) P. Rabe, Jap. J. Appl. Phys. 17, Suppl. 17-2, 22 (1978).
(18) P. Eisenberger and G.S. Brown, Solid State Commun. 29, 481 (1979).
(19) T.M. Hayes, J.B. Boyce and J.L. Beeby, J. Phys. C11, 2931 (1978).
(20) D.E. Polk and D.S. Boudreaux, Jour. de Phys. Colloque C2, 55 (1975).
(21) M. De Crescenzi, A. Balzarotti, F. Comin, L. Incoccia, S. Mobilio and N. Motta, Solid State Commun. 37, 921 (1981).
(22) E.D. Crozier and A.J. Seary, Can. J. Phys. 58 1388 (1980).
(23) E.D. Crozier, in: "EXAFS Spectroscopy" ed. by B.K. Teo and D.C. Joy (Plenum Press, N.Y. 1981).
(24) J.B. Boyce, T.M. Hayes and J.C. Mikkelsen Jr., Phys. Rev. B23, 2876 (1981).
(25) R. Haensel, P. Rabe, G. Tolkiehn and A. Werner, in: "Liquid and Amorphous Metals" ed. by E. Lüscher (D. Reidel, Dodrecht (1980)).
(26) See for a review: "Metallic Glasses" ed. by H. Guntherodt (Springer Verlag, Berlin) (1980).
(27) G.S. Gargill III, in: "Advances in Solid State Physics" ed. by H. Ehrenreich, F. Seitz and D. Turnbull, (Academic Press, N.Y. 1975).
(28) T.M. Hayes, J.W. Allen, J. Tauc, B.G. Giessen and J.J. Hauser, Phys. Rev. Letters 40, 1282 (1978).
(29) P. Lagarde, These proceedings.
(30) D.S. Boudreaux, Phys. Rev. B18, 4039 (1978).
(31) Y. Waseda and H.S. Chen, Solid State Commun. 27, 809 (1978).
(32) E. Sevillano, H. Meuth and J.J. Rehr, Phys. Rev. B20, 4908 (1979).